

# Accurate CSA measurements from uniformly isotopically labeled biomolecules at high magnetic field

Suzanne R. Kiihne\*, Alain F.L. Creemers, Johan Lugtenburg, Huub J.M. de Groot

*Leiden Institute of Chemistry, Gorlaeus Laboratories, P.O. Box 9502, 2300RA Leiden, The Netherlands*

Received 4 February 2004; revised 21 August 2004

## Abstract

Obtaining chemical shift anisotropy (CSA) principal values from large biomolecular systems is often a laborious process of preparing many singly isotopically labeled samples and performing multiple independent CSA measurements. We present CSA tensor principal values measured in the biomolecular building blocks tyrosine-HCl, histidine-HCl, and all-E-retinal in both isotopically labeled and unlabeled forms at 17.6 T. The measured tensor values are identical for most carbon sites despite significant dipolar couplings between the spins. Quantum mechanical simulations of an arbitrary three spin system were used to evaluate the accuracy of direct CSA measurement as a function of applied magnetic field strength and molecular parameters. It was found that for a CSA asymmetry of 0.2 or more, an accurate measure of the CSA parameters is obtained when the CSA anisotropy is more than six times the largest dipolar coupling in frequency units. If the CSA asymmetry is more than 0.5, this requirement is relaxed, and accurate results are obtained if the anisotropy is more than three times the dipolar coupling. While these limits are insufficient for measurement of CSA's for  $\alpha$ -carbons and aliphatic sidechain sites in proteins at current field strengths, they open the way for routine systematic CSA measurements of sites with relatively large CSA tensor values in extensively isotopically labeled biomolecules in widely available magnetic fields.

© 2004 Published by Elsevier Inc.

*Keywords:* Chemical shift anisotropy; Dipolar coupling; Magic angle spinning; Biological structure; High field

## 1. Introduction

Solid state NMR is a rapidly developing method for gaining detailed biophysical insight from systems that cannot be studied by solution state NMR or X-ray crystallography. Recent advances have made it possible to determine full 3D structures of uniformly  $^{13}\text{C}$  and  $^{15}\text{N}$  labeled biological solids through multidimensional methods [1–4]. Other approaches have allowed detailed studies of ligand–protein interactions [5]. Advantages in sensitivity and resolution, as well as advances in magnet design are leading solid state NMR to higher magnetic fields. These new experimental conditions have

significant implications for established experimental methods. Herein, we explore the high field limit of CSA tensor measurements in uniformly isotopically labeled biomolecules. The experimental and simulated results indicate that widely available magnetic field strengths are already sufficient for accurate measurements at many biologically interesting molecular sites.

Chemical shift scales with applied field strength, and thus, the anisotropic chemical shift and its cross terms with other quantum mechanical interactions are significantly larger at high magnetic fields. Sideband patterns observed by MAS NMR are distorted by dipolar couplings between adjacent spins in multiply isotopically labeled systems, skewing the results of CSA measurements. However, dipolar couplings do not scale with the applied field, and these distortions are reduced at high field,

\* Corresponding author. Fax: +31 71 527 4603.

E-mail address: [s.kiihne@chem.leidenuniv.nl](mailto:s.kiihne@chem.leidenuniv.nl) (S.R. Kiihne).

obviating the need for specialized methods of CSA measurement. In this report, we quantify the accuracy of direct, uncompensated CSA measurements in uniformly isotopically labeled biomolecules.

Dipolar recoupling methods are among the most versatile and widely used tools for structure determination by solid state NMR [6]. They employ RF pulses to reintroduce the dipolar couplings, which are otherwise averaged by MAS. In most homonuclear experiments, the results depend on the chemical shifts of the nuclei involved, and sensitivity to higher order chemical shift terms is considered the most important factor in performance variations at moderate field strengths [7]. The importance of these CSA terms increases at higher field, where poorly characterized CSA's become significant sources of error. Structural measurements involving molecular sites with relatively large CSA's are particularly sensitive to these effects. Some knowledge of the CSA is therefore necessary for accurate dipolar recoupling measurements in high magnetic fields.

For dipolar recoupling applications in peptide systems, *in situ* CSA measurements are usually avoided by using canonical values from reference studies of glycine and alanine in small peptides and in amino acid polymers [8,9]; however, the protein environment can influence the CSA, causing significant deviations from these canonical values. This is accepted to be the case for  $C_{\alpha}$  CSA's, which have recently been shown to correlate with the peptide backbone conformation [10], but it is also true for sidechain chemical shifts and for carbonyl CSA's, which reflect the strength of the hydrogen bond. An estimate of the normal CSA variation for any particular site can be obtained from the BioMagRes database [11]. Protein structures deposited in the database show an isotropic chemical shift range for the backbone C=O of nearly 25 ppm (165–189 ppm). Since the amide bond is planar and invariant, this indicates much larger variations in one or more of the anisotropic CSA parameters. For C=O, this is generally accepted to be primarily due to variations in  $\sigma_{22}$  [12]. Thus, normal variations in CSA can cover a significant frequency range at high magnetic fields, and relying on a single set of canonical values could be misleading. Additionally, for most non-peptide systems, including many biologically important ligands, aggregates, polysaccharides, and modified amino acids, canonical CSA values are not available.

A common, though laborious, approach to this problem has been to prepare a variety of singly isotopically labeled samples and to obtain many independent CSA measurements [13]. With the recent introduction of dipolar compensated CSA measurement methods, CSA's can now be measured in uniformly isotopically labeled systems [14]. For large CSA's, however, these new methods require fast spinning and extremely high RF power levels. This makes them inappropriate for delicate

biological samples, including membrane proteins. Herein, we demonstrate that direct high field measurement of larger CSA tensors in uniformly isotopically labeled samples by existing techniques often yields accurate results, even without dipolar compensation. Through simulations, we further explore and quantitate the limits of this high field effect.

CSA measurements on multispin systems involve crowded spectra, and are best measured by multidimensional methods. Many approaches are now available, including magic angle turning approaches such as FIREMAT and its relatives [15], and MAS methods based on TOSS and PASS [16,17]. More recently, techniques for measuring chemical shift powder patterns or enhanced powder patterns under (fast) MAS conditions have been developed [14,18]. In all these methods, the isotropic and anisotropic parts of the chemical shift are separated into two dimensions. Methods that separate the spinning sidebands by order instead of frequency accomplish this separation with a minimum number of  $t_1$  slices, reducing the measurement time. Using uncompensated methods in multiply isotopically labeled systems with significant dipolar couplings requires some consideration of the pulse sequence length and of the nature of the applied RF fields. We have chosen to use 2D PASS because of its short, constant time pulse sequence, and its minimal number of  $t_1$  slices [17].

## 2. Experimental methods

### 2.1. Samples

Unlabeled tyrosine, valine, and histidine were obtained from Sigma.  $U\text{-}^{13}\text{C}$ ,  $^{15}\text{N}$ -tyrosine and  $U\text{-}^{13}\text{C}$ ,  $^{15}\text{N}$ -histidine were obtained from CIL. Tyrosine and histidine samples were recrystallized from water at pH 7.0 containing equimolar HCl to form the hydrochloride salts. Unlabeled all-E-retinal was obtained from Sigma and used without further purification. [ $U\text{-}^{13}\text{C}$ ]all-E-retinal was synthesized by total synthesis [19]. The all-E conformer was isolated by HPLC with 25% diethyl ether in petroleum ether. The total amount isolated was determined by UV-vis spectroscopy assuming an extinction coefficient,  $\epsilon = 48,900$  at 368 nm in pentane. To suppress intermolecular dipolar couplings, uniformly labeled retinal was diluted to 6% with natural abundance material before crystallization from pentane at  $-80^\circ\text{C}$ . All samples were packed into 4 mm zirconium rotors. The structures and numbering schemes are shown in Fig. 1.

### 2.2. Solid state NMR

NMR experiments were recorded with an Avance-WB750 spectrometer, equipped with a 4 mm triple reso-

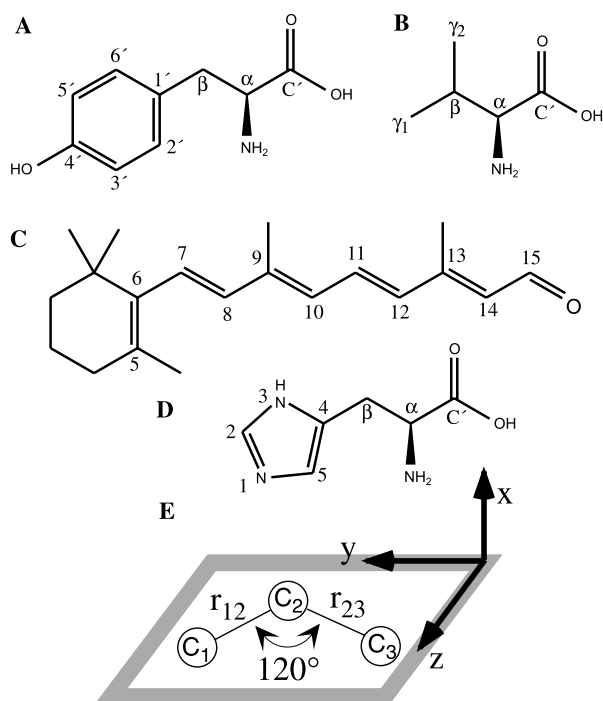


Fig. 1. Numbering systems. (A–D) Numbering of the molecules tyrosine, valine, all-E-retinal, and histidine, respectively. (E) The model system geometry used for simulations. The  $z$ -axis of the molecular frame bisects the  $C_1$ – $C_2$ – $C_3$  angle.

nance CP/MAS probe (Bruker, Karlsruhe, Germany). The ‘nonlinear’ PASS experiment provided in the Bruker software release was used with the full 243 step phase cycle [17]. The  $^1\text{H}$  power was ramped 100–50% during CP. The  $^{13}\text{C}$   $180^\circ$  pulses varied between 6 and 8  $\mu\text{s}$  in different experiments. This variation did not affect the observed sideband patterns.  $^1\text{H}$  decoupling was about 120 kHz CW during the PASS sequence and 81 kHz TPPM during acquisition [20]. Sixteen  $t_1$  slices were acquired in all cases. Decoupling was not interrupted during the PASS pulses, as this did not appear to affect the observed sideband patterns. The RF irradiation was centered in the region of interest to minimize the effects of pulse imperfections.

### 2.3. Data processing

Spectra were processed with line broadening in  $t_2$ , no windowing in  $t_1$ . Better results were obtained when the 1st point of the FID was not multiplied by 0.5 [17]. Multiplying by 0.5 led to  $t_1$  ridges. A cosine transform was used in  $t_1$ . The Bruker command ‘ptilt’ was used to align the sidebands in the second dimension of the 2D spectrum. Integrated intensities were obtained by simple summation over all  $t_2$  points with significant signal to noise for each sideband. Noise was measured by a similar summation over a nearby part of the spectrum, which did not contain any visible signals. Alternatively, NMRPipe [21] was used to transform the data, after

which it was loaded into Matlab (Mathworks) for trapezoidal integration over the sideband and noise regions. Results of these two approaches were comparable.

CSA parameters were extracted from the peak volumes using a fitting procedure based on the approach of Antzutkin et al. [22]. Each fit required about 30 s on a Macintosh G4 using homemade routines written in Matlab 5.0 (see Supporting information). CSA values obtained for the carbonyl peak of glycine with these methods were consistent with literature values [23]. For comparison, principal axis values in literature references were converted to  $\delta$  and  $\eta$  by using the definitions:  $\delta = \sigma_{zz} - \sigma_{\text{iso}}$ ,  $\eta = \sigma_{xx} - \sigma_{yy} / \sigma_{zz} - \sigma_{\text{iso}}$ .

### 2.4. Simulation methods

Simulations were used to explore the effects of dipolar couplings on the observed spinning sideband patterns as a function of important experimental and molecular parameters. Simulations were carried out in Matlab 5.0 with home made routines that used Gaussian spherical quadrature [24] to calculate the spectrum obtained from a three-spin system. The molecular geometry shown in Fig. 1E was used in all simulations. The three spins are arranged as for an arbitrary chain of  $\text{sp}^2$  carbons with a  $120^\circ$  bond angle. The simulations include the CSA on the central carbon and two dipolar couplings, collinear with the bonds. The molecular frame is defined as shown with the  $z$ - and  $y$ -axes in the plane of the spins and the  $x$ -axis pointing out of the page. To reduce the dimensionality of the variable space and to allow direct comparison of sideband patterns at different applied magnetic fields, CSA’s and spin rates, a reduced CSA anisotropy parameter,  $\delta_{\text{aniso}}$ , was fixed at a constant value. This scaled anisotropy is defined as  $\delta_{\text{aniso}} = \delta_{\text{aniso}} / \delta_r$  where  $\delta_{\text{aniso}}$  and  $\delta_r$  are the anisotropy and spin rate, respectively, expressed in frequency units. (see supporting information).

### 3. Experimental results

The 2D PASS spectrum of  $[\text{U-}^{13}\text{C}]$ all-E-retinal obtained at 188 MHz  $^{13}\text{C}$  resonance frequency and 6000 Hz spinning frequency is shown in Fig. 2. A well resolved NMR spectrum is observed at this field and spin rate, despite the uniform isotopic labeling. The sideband manifolds of peaks near the center of the spectrum are well separated in  $t_1$  by the PASS experiment, with some remaining overlap due to insufficient dispersion of the isotropic shifts in  $t_2$ . The aliphatic signals were poorly refocused due to their large chemical shift offsets, leading to artefacts at the edges of the very broad spectral width, well separated from the sidebands of interest.

Good fits with  $\chi^2 \leq (n - 2)$ , where  $n$  is the number of data points, were obtained for all chemical sites with

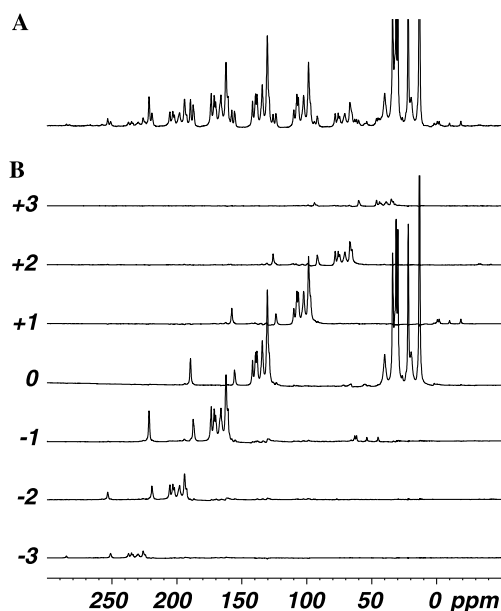


Fig. 2. Experimental results from 2D PASS experiment on U-<sup>13</sup>C-tyrosine-HCl at 750 MHz, 6 kHz spin rate. The corresponding 1D spectrum is shown above.

CSA's larger than 70 ppm in the samples studied. Experimental data (gray bars) and the best fit simulation (black line) obtained for the C8 position of [U-<sup>13</sup>C]all-E-retinal are shown in Fig. 3A. The experimental data and optimal fits obtained from the labeled and unlabeled systems were essentially indistinguishable. The results obtained from other sites and molecules are summarized by the correlation plots in Figs. 3B and C for  $\delta$  and  $\eta$ , respectively. The correlations between results obtained for these resolved sites in labeled and unlabeled materials are quite good, and show deviations of  $\leq 3$  ppm in  $\delta$  and  $\leq 0.1$  in  $\eta$  between the uniformly <sup>13</sup>C labeled and unlabeled materials. The solid lines shown in Figs. 3B and C represents exact 1:1 correspondence between the measurements and are simply shown to guide the eye. Variations between measurements at different spin rates were usually larger than those between samples with different labeling schemes. The measured CSA values are summarized and compared to literature results in Table 1.

These results show that uncompensated CSA measurements provide good estimates of the chemical shift tensor parameters for molecular sites with relatively large CSAs in uniformly <sup>13</sup>C labeled systems at high field. Attempts to measure CSA's in U-<sup>13</sup>C-L-glucose and at the C $\beta$  position in U-<sup>13</sup>C, <sup>15</sup>N-tyrosine-HCl were unsuccessful because the sideband manifolds could not be resolved at the spin rates required for direct CSA measurement. Spin rates required for measurement of the C $\alpha$  chemical shift anisotropy were close to the C $\alpha$ -C $\beta$  rotational resonance condition and displayed additional broadening.

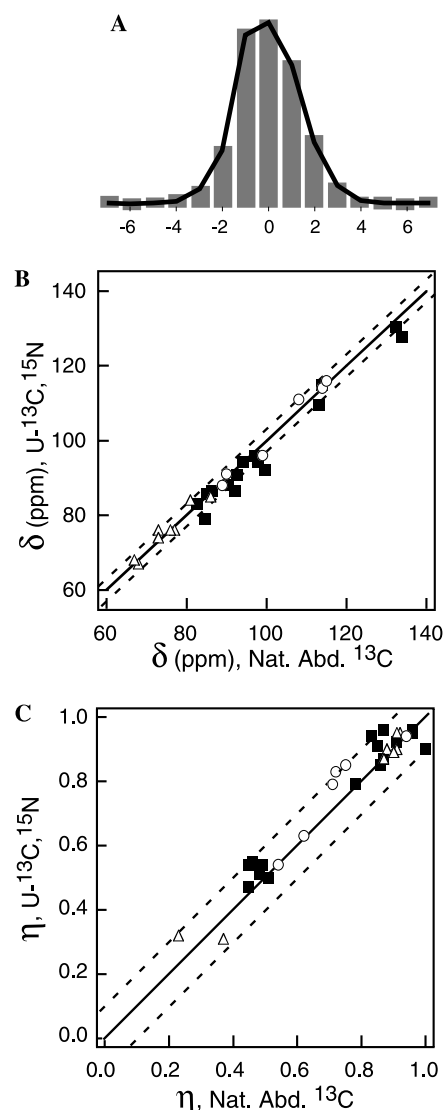


Fig. 3. Fitting and experimental results. Experimental sideband intensities (gray bars) and the best simulated fit (black line) for the C8 position of [U-<sup>13</sup>C]all-E-retinal are shown in (A). The spin rate was 6 kHz at 188 MHz. The fitting procedure yielded  $\delta_{\text{aniso}} = -2.72$  for both cases, and  $\eta = 0.85$  and  $0.86$  for the unlabeled and uniformly <sup>13</sup>C labeled systems, respectively. The final  $\chi^2$  was 8.7 ( $n = 15$ ). (B and C) Correlation plots of experimentally determined  $\delta$  and  $\eta$  values obtained from natural abundance and uniformly isotopically labeled samples, respectively at spin rates of 4–6.5 kHz. Black squares, retinal; white triangles, histidine-HCl:H<sub>2</sub>O; and white circles, tyrosine-HCl. The solid line represents 1:1 correspondence between the two measurements. The dotted lines represent error limits of  $\pm 3$  ppm and  $\pm 0.1$  in the anisotropy and asymmetry, respectively.

#### 4. Results of simulations

Simulated sideband manifolds for a dipolar coupled three spin system are shown in Fig. 4. In the absence of dipolar couplings, the sideband patterns would be identical. Comparison of the envelopes of sideband signal intensity shown in gray indicates that, as the field strength increases, the mixed dipolar/CSA sideband

Table 1  
Chemical shift anisotropies and literature values

	$\sigma_{\text{iso}}$	$\sigma_{\text{iso}}$ (ref)	$\delta$	$\delta$ (ref)	$\eta$	$\eta$ (ref)
<b>Retinal</b>						
5	128.5	129.3	100	98	0.72	0.76
6	139.1	141.0	93	90	0.89	0.98
7	130.1	129.0	91	90	0.87	0.88
8	138.0	142.6	87	84	0.87	0.95
9	141.3	143.1	108	110	0.69	0.54
10	130.1	130.4	79	81	0.99	0.99
11	134.0	130.8	102	102	0.94	0.77
12	134.0	133.9	82	82	0.99	0.93
13	155.3	152.6	130	125	0.56	0.50
14	130.1	130.9	72	70	0.93	1.00
15	188.2	190.1	95	92	0.54	0.51
<b>Histidine-HCl</b>						
CO	173		67		0.95	
$\epsilon$	133		85		0.30	
$\gamma$	126		76		0.90	
$\delta$	119		75		0.90	
<b>Tyrosine-HCl</b>						
CO	172.2		89		0.54	
1	125.0		-114		0.72	
2	133.0		-107		0.75	
3	114.0		-94		0.72	
4	151.8		90		0.94	
5	117.5		-99		0.62	
6	129.5		-115		0.71	
<b>Valine</b>						
$\gamma_1$	20.70	22.1	-18	-24	0.74	0.56
$\gamma_2$	17.20	19.2	-15	24	0.26	0.31

Literature values are from references [13] and [23] for retinal and valine, respectively.

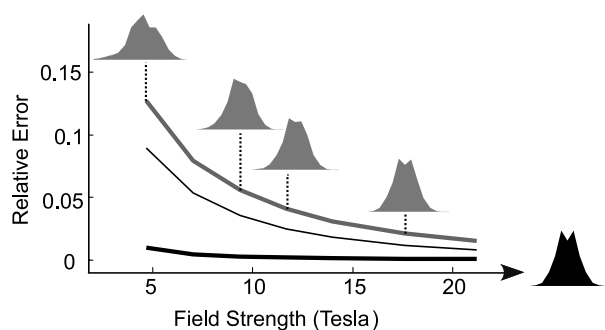


Fig. 4. Comparison of simulated dipolar coupled and CSA-only sideband patterns at different field strengths. Simulations were based on the three spin system shown in Fig. 1E. The C2 CSA was set to  $(\delta, \eta) = (-130.5, 1.0)$ . The CSA and dipolar tensors were transformed to the molecular frame using  $\Omega^{\text{CSA}}(\alpha, \beta, \gamma) = (90, -90, 0)$  and  $\Omega^{\text{D}}(\alpha, \beta, \gamma) = (0, \pm 60, 90)$ , respectively. Wide gray, narrow black, and wide black lines correspond to equal  $r_{12} = r_{23} = 135, 150,$  and  $240$  pm, respectively. The spin rate was varied with the applied field strength so that  $\delta_{\text{aniso}} = 3.3$ . The sideband patterns would be identical in the absence of dipolar couplings. Signal intensity envelopes for sideband patterns calculated with  $r_{12} = r_{23} = 135$  pm are shown in gray at field strengths of 4.7, 9.4, 11.7, and 17.6 T. The CSA-only sideband pattern is shown in black.

manifold approaches the CSA-only envelope shown in black. The lines in Fig. 4 show the relative error between the mixed dipolar/CSA and CSA-only sideband patterns

for a series of bond lengths and magnetic fields. The relative error is calculated as the sum of the squared deviations between the two simulated sideband patterns, normalized to the square of the total intensity of the CSA-only sideband pattern. As expected, the distortions due to dipolar couplings decrease at higher fields. For directly bonded carbons, the deviation from the unperturbed spinning sideband pattern is less than 5% at a field strength of 10 T or higher, but rises steeply at lower fields.

Further simulations were carried out to explore the limits of this approach with respect to dipolar coupling strength, CSA anisotropy, asymmetry, and tensor orientation in the molecular frame. A detailed discussion is given as Supporting information, and the results are summarized here. From the simulations, it appears that the applicability of this method depends somewhat on the CSA parameters being measured. Specifically, while the dipolar coupling strength is the main limitation, the asymmetry parameter of the measured CSA is an important factor. In the absence of dipolar couplings, our results confirm that small values of  $\eta$  are difficult to measure accurately under MAS conditions [25]. In the presence of dipolar couplings, this problem is magnified, and large errors in both  $\delta$  and  $\eta$  are observed with small

input values of  $\eta$ . The relative importance of these errors depends on the dipolar coupling strength. The simulations also show that the relative CSA tensor orientation in the molecular frame has a relatively small influence on the CSA measurement error.

## 5. Discussion

The results show that accurate CSA tensor values can be obtained from uniformly isotopically labeled biomolecules at high magnetic field by simple methods that do not actively compensate for dipolar couplings. Experimentally measured CSA values from unlabeled and uniformly  $^{13}\text{C}$  labeled tyrosine-HCl, histidine-HCl, and all-E-retinal were identical to within  $\pm 3$  ppm in  $\delta$  and  $\pm 0.1$  in  $\eta$  for all sites that could be resolved by the 2D PASS application at a  $^{13}\text{C}$  resonant frequency of 188 MHz. These experimental results are consistent with simulations of a system of three dipolar coupled spins, which show that the distortions in CSA sideband patterns observed in high magnetic field due to single-bond dipolar couplings are quite small. Together, the simulations and experiments indicate that accurate tensor values can be obtained for biologically interesting molecular sites at widely available magnetic fields.

We were not able to extend this experimental approach to all molecular sites in the systems studied because of limited resolution in the 1D spectra. This resolution limitation was primarily due to the dipolar couplings between nearest neighbor carbons, which cause significant peak broadening at the slow MAS rates needed to measure smaller CSA tensors with the methods used. CSA's with an anisotropy larger than approximately 70 ppm in a field of 17.6 T could be measured with the 2D PASS method. The technique proposed recently by Chan and Tycko [14] can be used for measuring smaller CSA tensors. That technique is optimised for such systems, but is less successful in measuring large CSA's. The two methods appear to be complementary in this respect.

The three-spin simulations indicate that this method is applicable to a range of molecular sites at moderate fields. At 17.6 T, the simulations indicate that a  $^{13}\text{C}$  CSA tensor with an anisotropy of 75 ppm or more can be measured with negligible error ( $d_{\text{max}} = 0.5$ ), in agreement with the experimental results. At 9.4 T, these simulations predict that large  $^{13}\text{C}$  CSA tensors of  $\delta > 140$  ppm can be measured with negligible error. Additionally,  $^{13}\text{C}$  CSA tensors with  $\delta$  as small as 70 ppm can be measured accurately at 9.4 T, so long  $\eta$  is greater than 0.5. This includes all known peptide carbonyls, and most aromatic sidechain resonances. We have verified this by comparing experimental measurements of the carbonyl and aromatic sites in labeled and unlabeled histidine at 9.4 T. The results agree with

those in Table 1 (data not shown). These observations can be generalized by noting that small errors of  $< 3\%$  in  $\delta$  and  $< 0.1$  in  $\eta$  are achieved for tensors with  $\eta > 0.2$  so long as the CSA anisotropy,  $\delta$ , is more than six times the strongest dipolar coupling. When  $\eta$  is  $> 0.5$ , this requirement is relaxed, and  $\delta$  need only be three times the strongest dipolar coupling in frequency units.

The PASS experiment is sensitive to pulse imperfections. These imperfections were minimized here by using the long 243 step PASS phase cycle [17]. New developments with cogwheel phase cycling promise to make this process significantly more efficient [26]. In our case, the problem of pulse imperfections is exacerbated by the fast spin rates used at high field, and non-ideal pulse effects are probably the single largest source of experimental error. This source of error was equal for measurements in the uniformly labeled and unlabeled systems, and may explain the differences between measurements made at different spin rates. Nevertheless, the experimental CSA values reported in Table 1 are very close to the reference values, suggesting that these errors are less than 5%.

Sideband intensity distortions caused by dipolar couplings lead to systematic errors in the CSA parameters obtained by fitting to a CSA-only sideband pattern. The three spin simulations reported in Fig. 4 and in the Supporting information give an indication of the magnitude of these errors as a function of the applied magnetic field strength and molecular parameters. The total error is the geometric sum of the independent errors in the measurement. With the uncompensated method described here, there are three main sources of error: systematic errors due to pulse imperfections, systematic errors due to the dipolar couplings, and random errors due to spectral noise. In systems with random noise on the order of 5–8%, an additional 3–5% systematic error induced by this direct approach may be superior to the available alternatives.

This is a very useful observation for future MAS NMR investigations. Chemical shift anisotropies contain information that is often complementary to that obtained from isotropic chemical shifts. Previously, such information has been gained from experiments on a series of samples containing isolated isotope labels. Our results show that this laborious approach is often unnecessary, because accurate measurements can be obtained for many sites simultaneously in uniformly isotopically labeled systems by simple, robust methods. This ability to efficiently obtain extensive, accurate CSA information from uniformly or partially uniformly isotopically labeled materials removes a bottleneck to routine, systematic CSA measurements. We expect that broad implementation of this and complementary approaches [14] will yield further insight into specific CSA/structure relationships, particularly in proteins

and peptides where structural motifs are efficiently recycled. Developing a predictive library of  $^{15}\text{N}$  CSA tensors has been proposed previously [27]. The efficient experimental approach for CSA measurements described herein makes this a realizable goal.

## 6. Conclusions

Accurate CSA tensor measurements in uniformly isotopically biomolecules are feasible at currently available magnetic fields. Experimental results from high field 2D PASS measurements of CSA tensor values in unlabeled and in uniformly labeled biomolecular building blocks were shown to be identical within the noise of the measurement for sites with  $\delta > 70$  ppm. The general applicability of this approach was explored in a series of three-spin simulations for an arbitrary CSA tensor in a dipolar coupled  $\text{sp}^2$  carbon chain over reduced experimental parameters. From these simulations, the expected errors in the anisotropy,  $\varepsilon(\delta)$ , and the asymmetry,  $\varepsilon(\eta)$ , were estimated. These results can be interpreted for applications in any system of spin 1/2 nuclei at any field strength. For uniformly labeled  $^{13}\text{C}$  systems, the simulations indicated that CSA's with  $\delta > 70$  ppm and  $\eta > 0.5$  can be measured with errors  $\varepsilon(\delta) < 5\%$  and  $\varepsilon(\eta) < 0.1$  at the commonly available field strength of 9.4 T. At a field of 17.6 T, CSA's with  $\delta > 38$  ppm and  $\eta > 0.5$  can be obtained with similar accuracy. These observations open the way for routine systematic measurement of CSA tensor values in isotopically labeled biomolecules. Such information is expected to lead to useful correlations between CSA and structure in peptides and proteins and to improve the accuracy of structure measurements by dipolar recoupling methods.

## Appendix. Supplementary material

Supplementary data associated with this article can be found, in the online version, at [doi:10.1016/j.jmr.2004.09.001](https://doi.org/10.1016/j.jmr.2004.09.001).

## References

- [1] B.J. van Rossum, E.A.M. Schulten, J. Raap, H. Oschkinat, H.J.M. de Groot, A 3-D structural model of solid self-assembled chlorophyll a/H<sub>2</sub>O from multispin labeling and MAS NMR 2-D dipolar correlation spectroscopy in high magnetic field, *J. Magn. Reson.* 155 (2002) 1–14.
- [2] F. Castellani, B. van Rossum, A. Diehl, M. Schubert, K. Rehbein, H. Oschkinat, Structure of a protein determined by solid-state magic-angle-spinning NMR spectroscopy, *Nature* 420 (2002) 98–102.
- [3] C.M. Rienstra, L. Tucker-Kellogg, C.P. Jaroniec, M. Hohwy, B. Reif, M.T. McMahon, B. Tidor, T. Lozano-Perez, R.G. Griffin, De novo determination of peptide structure with solid-state magic-angle spinning NMR spectroscopy, *Proc. Natl. Acad. Sci. USA* 99 (2002) 10260–10265.
- [4] S.J. Kim, L. Cegelski, D.R. Studelska, R.D. O'Connor, A.K. Mehta, J. Schaefer, Rotational-echo double resonance characterization of vancomycin binding sites in *Staphylococcus aureus*, *Biochemistry* 41 (2002) 6967–6977.
- [5] A.F.L. Creemers, S. Kiihne, P.H.M. Bovee-Geurts, W.J. DeGrip, J. Lugtenburg, H.J.M. de Groot, H-1 and C-13 MAS NMR evidence for pronounced ligand–protein interactions involving the ionone ring of the retinylidene chromophore in rhodopsin, *Proc. Natl. Acad. Sci. USA* 99 (2002) 9101–9106.
- [6] M. Baldus, Correlation experiments for assignment and structure elucidation of immobilized polypeptides under magic angle spinning, *Prog. NMR Spec.* 41 (2002) 1–47.
- [7] T. Karlsson, J.M. Popham, J.R. Long, N. Oyler, G.P. Drobny, A study of homonuclear dipolar recoupling pulse sequences in solid-state nuclear magnetic resonance, *J. Am. Chem. Soc.* 125 (2003) 7394–7407.
- [8] R. Tycko, Biomolecular solid state NMR: advances in structural methodology and applications to peptide and protein fibrils, *Ann. Rev. Phys. Chem.* 52 (2001) 575–606.
- [9] T.G. Oas, C.J. Hartzell, T.J. McMahon, G.P. Drobny, F.W. Dahlquist, The carbonyl  $^{13}\text{C}$  chemical shift tensors in five peptides determined from  $^{15}\text{N}$  dipole coupled chemical shift powder patterns, *J. Am. Chem. Soc.* 109 (1987) 5956–5962.
- [10] M. Hong, Solid-state NMR determination of C-13 alpha chemical shift anisotropies for the identification of protein secondary structure, *J. Am. Chem. Soc.* 122 (2000) 3762–3770.
- [11] BioMagRes data bank, 2004. Available from: <[bmr.b.wisc.edu](http://bmr.b.wisc.edu)>.
- [12] Z.T. Gu, R. Zambrano, A. McDermott, Hydrogen-bonding of carboxyl groups in solid-state amino-acids and peptides—comparison of carbon chemical shielding, infrared frequencies, and structures, *J. Am. Chem. Soc.* 116 (1994) 6368–6372.
- [13] G.S. Harbison, S.O. Smith, J.A. Pardo, J.M.L. Courtin, J. Lugtenburg, J. Herzfeld, R.A. Mathies, R.G. Griffin, Solid state  $^{13}\text{C}$  NMR detection of a perturbed 6-s-trans chromophore in bacteriorhodopsin, *Biochemistry* 24 (1985) 6955–6962.
- [14] J.C.C. Chan, R. Tycko, Recoupling of chemical shift anisotropies in solid-state NMR under high-speed magic-angle spinning and in uniformly C-13-labeled systems, *J. Chem. Phys.* 118 (2003) 8378–8389.
- [15] J.Z. Hu, A.M. Orendt, D.W. Alderman, R.J. Pugmire, C.H. Ye, D.M. Grant, Measurement of C-13 chemical-shift tensor principal values with a magic-angle turning experiment, *Solid State Nucl. Magn. Reson.* 3 (1994) 181–197.
- [16] W.T. Dixon, Spinning-sideband-free and spinning-sideband-only NMR spectra in spinning samples, *J. Chem. Phys.* 77 (1982) 1800–1809.
- [17] O.N. Antzutkin, S.C. Shekar, M.H. Levitt, Two-dimensional sideband separation in magic-angle spinning NMR, *J. Magn. Reson. A* 115 (1995) 7–19.
- [18] S.F. Liu, J.D. Mao, K. Schmidt-Rohr, A robust technique for two-dimensional separation of undistorted chemical-shift anisotropy powder patterns in magic-angle-spinning NMR, *J. Magn. Reson.* 155 (2002) 15–28.
- [19] A.F.L. Creemers, J. Lugtenburg, The preparation of all-trans uniformly C-13-labeled retinal via a modular total organic synthetic strategy. Emerging central contribution of organic synthesis toward the structure and function study with atomic resolution in protein research, *J. Am. Chem. Soc.* 124 (2002) 6324–6334.
- [20] A.E. Bennett, C.M. Rienstra, M. Auger, K.V. Lakshmi, R.G. Griffin, Heteronuclear decoupling in rotating solids, *J. Chem. Phys.* 103 (1995) 6951–6958.
- [21] F. Delaglio, S. Grzesiek, G.W. Vuister, G. Zhu, J. Pfeifer, A. Bax, NMRPipe: a multidimensional spectral processing system based on UNIX pipes, *J. Biomolecular NMR* 6 (1995) 277–293.

- [22] O.N. Antzutkin, Y.K. Lee, M.H. Levitt, C-13 and N-15 chemical shift anisotropy of ampicillin and penicillin-V studied by 2D-PASS and CP/MAS NMR, *J. Magn. Reson.* 135 (1998) 144–155.
- [23] C. Ye, R. Fu, J. Hu, L. Hou, S. Ding, Carbon-13 chemical shift anisotropies of solid amino acids, *Magn. Reson. Chem.* 31 (1993) 699–704.
- [24] M. Eden, M.H. Levitt, Computation of orientational averages in solid-state NMR by Gaussian spherical quadrature, *J. Magn. Reson.* 132 (1998) 220–239.
- [25] P. Hodgkinson, L. Emsley, The reliability of the determination of tensor parameters by solid-state nuclear magnetic resonance, *J. Chem. Phys.* 107 (1997) 4808–4816.
- [26] N. Ivchenko, C.E. Hughes, M.H. Levitt, Application of cogwheel phase cycling to sideband manipulation experiments in solid-state NMR, *J. Magn. Reson.* 164 (2003) 286–293.
- [27] Z.T. Gu, A. McDermott, Chemical shielding anisotropy of protonated and deprotonated carboxylates in amino-acids, *J. Am. Chem. Soc.* 115 (1993) 4282–4285.